Towards entropy-driven interstitial micelles at elevated temperatures from selective $A1BA2$ triblock solutions

S. Wołoszczuk
Faculty of Physics, Adam Mickiewicz University, ulica Umultowska 85, 61-614 Poznan, Poland

S. Jurga
Department of Macromolecular Physics, NanoBioMedical Centre, Adam Mickiewicz University, ulica Umultowska 85, 61-614 Poznan, Poland

M. Banaszak*
Faculty of Physics, Adam Mickiewicz University, ulica Umultowska 85, 61-614 Poznan, Poland
(Received 17 April 2016; revised manuscript received 30 May 2016; published 29 August 2016)

We simulate selective $A1BA2$-A and $A1BA2$-B triblock solutions (that is, mixtures of the $A1BA2$ triblock with a solvent of either type A or type B) using a lattice Monte Carlo method. Although the simulated triblock chains are compositionally symmetric in terms of the A to B volume ratio, the $A1$ block is significantly shorter than the $A2$ block. For the pure $A1BA2$ melt the phase behavior is relatively well known, including the existence and stability of the recently discovered interstitial micelles which were found at the very strong segregation limit. In this paper, we investigate the stability of the interstitial micelles as a function of triblock volume fraction in a selective solvent of either type A or type B. The main finding of this paper is that adding a selective solvent of type A shifts the stability of the interstitial micelles into significantly higher temperatures which may provide a pathway towards experimental studies of interstitial micelles in real triblock solutions. We also find that adding selective solvents to the $A1BA2$ melt gives rise to a variety of nonlamellar nanostructures for temperatures and compositions at which the interstitial micelles are stable.

DOI: 10.1103/PhysRevE.94.022502

I. INTRODUCTION

Block copolymers are extensively studied due to their intrinsic ability to self-organize spontaneously into a wide variety of periodic nanostructures, to compatibilize immiscible polymers, and to locate at polymer-polymer interfaces [1–12]. These intriguing soft materials can form nanostructures upon microphase separation which occurs via an order-disorder transition (ODT). Furthermore, order-order transitions (OOT) are observed between different self-assembled morphologies. In this paper, we focus our attention exclusively on ABA triblock solutions by extending the scope of a previous paper [13] and specifying a new goal.

In a previous paper [13], we examined pure triblock melts employing lattice Monte Carlo (MC) simulations and, selectively, using dissipative particle dynamics. We explored the phase behavior of molecularly asymmetric $A1BA2$ copolymers possessing chemically identical end blocks ($A1$ and $A2$) but differing significantly in length. It is well known that the midblock bridging fraction determines the bulk mechanical properties in triblock copolymers in the melt [14–17] as well as in the presence of a selective solvent [18]. In this case, each copolymer chain can be classified as a bridge (each A end block resides in a different A microdomain), a loop (both A end blocks locate within the same A microdomain), a dangle (one A end block sits in an A microdomain whereas the other remains in the B matrix), or mixed (both A end blocks stay within the B matrix). Dangles can be preferentially formed if the ABA triblock contains the same volume of A and B, but one of the A end blocks is much shorter than the other. At the same composition at which the fraction of dangles is high, the bridging fraction is low, and this may impair the network formation because the A network is spanned by the ABA bridges. It is, therefore, interesting and potentially useful (for controlling bulk mechanical properties) that the short A blocks which form dangles can further self-assemble into A micelles with the B matrix as demonstrated for the first time in Ref. [13]. In particular, we showed [13] the existence of two different modes of self-assembly in a compositionally symmetric (i.e., 50:50 A:B) 46-48-2 copolymer. The long terminal blocks formed the primary morphology composed of lamellar microdomains, whereas the short A end blocks organized into a secondary morphology designated as interstitial micelles (IMs), localized along the midplane of the B lamella. In this manner IMs may contribute to a novel mechanism of bridging via the following sequence: long terminal block, midblock, interstitial micelle composed of many short terminal blocks, midblock, and long terminal block as indicated in Fig. 1; note that selected midblocks of type B blocks are shown in green (light gray).

Simulations established the molecular-asymmetry and incompatibility conditions under which such micelles formed as well as the temperature dependence of their aggregation number. Beyond an optimal length of the $A1$ end block, the propensity for IMs to develop decreased, and the likelihood for collocation of both end blocks in the $A2$-rich lamellae increased. Moreover, in pure triblock melts, the IMs were stable at very strong segregations which correspond to either very low temperatures or very long chains. This poses an experimental challenge for the IM formation because polymers become glassy at low temperatures, and they do not reach

*mbanasz@amu.edu.pl

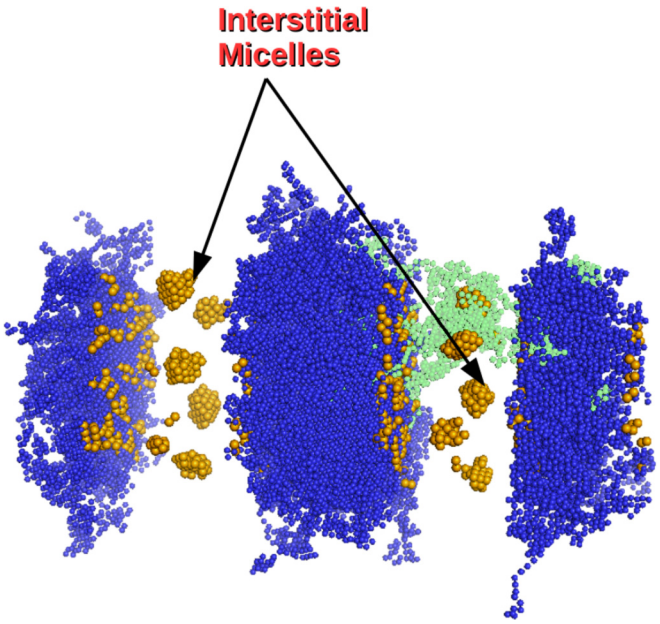

FIG. 1. Snapshot from a simulation of the $A_2 - B_{48} - A_{46}$ melt at $T^* = 1.7$ which shows interstitial micelles. Long $A2$ blocks are shown in blue (dark gray), short $A1$ blocks are shown in yellow (medium gray), and selected B blocks are shown in green (light gray); we show only those B blocks that are connected to the upper-right interstitial micelle.

the thermal equilibrium state if they have excessive molecular weights. In this paper, we intend to study the $A1BA2$ solutions in a selective solvent of either type A or type B in order to explore an experimental strategy for establishing optimal conditions for the IM formation. It is worthwhile to underline that this was not explored experimentally either for melts or for solutions and that IMs were found only in simulations so far. We expect that adding a selective solvent will significantly increase the temperature at which IMs are formed and therefore also decrease the thermodynamic incompatibility parameter χN (where χ is the Flory interaction parameter and N is the polymer chain length).

II. METHOD

The cooperative motion algorithm [17,19–22], based on a face centered cubic (fcc) lattice, is used to simulate the triblock solutions. We apply standard MC simulations with the Metropolis algorithm [23] as well as the parallel tempering (PT) method [24,25]. In the PT case, M replicas of systems are simulated in parallel, each in different temperature T_i's with i ranging from 1 to M. After 3000 MC steps we try to exchange replicas with neighboring T_i's in random order with probability,

$$p(T_i \leftrightarrow T_{i+1}) = \min\{1, \exp[-(\beta_i - \beta_{i+1})(U_{i+1} - U_i)]\}, \quad (1)$$

where $\beta_i = 1/kT_i$ and U_i is the potential energy of the replica at T_i. This method offers efficient equilibration at low temperatures.

We repeat the experiment at least three times starting with different initial configurations in which the polymer chains assume statistical conformations and random orientations and are uniformly distributed within the simulation box. A single MC step is defined as an attempt to move a given segment. Usually, the first half of the run is used to equilibrate the system, and the second one is used to collect the data. The results are averaged over all simulation runs. Although the morphologies obtained in the simulations were quantitatively dependent on the box size, this dependence was weak and did not change the main conclusions qualitatively.

We use the following set of interaction energies which are limited to the nearest neighbors,

$$\epsilon_{AB} = \epsilon, \quad (2)$$

$$\epsilon_{AA} = 0, \quad (3)$$

$$\epsilon_{BB} = 0, \quad (4)$$

where ϵ is an energy unit and we define the reduced energy per lattice site and the reduced temperature as

$$\frac{E^*}{n_a} = \frac{E/\epsilon}{n_a}, \quad (5)$$

$$T^* = \frac{kT}{\epsilon}. \quad (6)$$

On the basis of considerations presented in Ref. [26], we can relate T^* used in this paper to the Flory χ parameter employed in the self-consistent field theory [27] by the following approximate equation:

$$\chi = \frac{7.5}{T^*}. \quad (7)$$

The above equation can also be used in order to relate theoretical T^*'s to experimental χ's. Although we do not provide any direct link to experimental data in this paper, it is well established that the method that we use gives at least a qualitative agreement with the experimental data as, for example, the order-disorder temperature depression for highly asymmetric polystyrene-polyisoprene-polystyrene triblocks [28] and surprising phase diagrams for nearly symmetric poly-(styrenesulfonate)-polymethylbutylene (PSS-PMB) [26] also for asymmetric PSS-PMB [29].

The heat capacity C_v is calculated from the energy fluctuations as follows:

$$\frac{C_v}{n_a} = \frac{\langle (E^* - \langle E^* \rangle)^2 \rangle}{n_a T^{*2}}. \quad (8)$$

We also calculate the structure factor $[S(k)]$ using the following equation:

$$S(\vec{k}) = \frac{1}{n_\alpha} \left\langle \left(\sum_{m=1}^{n_\alpha} \cos(\vec{k} \cdot \vec{r}_m) \right)^2 + \left(\sum_{m=1}^{n_\alpha} \sin(\vec{k} \cdot \vec{r}_m) \right)^2 \right\rangle_{\text{thermal average}}, \quad (9)$$

where n_α is the number of segments of type α and $\vec{r}_m$ is the position of the mth segment of type α. The wave vectors $\vec{k}$ are commensurate with the simulation box size, and this constraint limits their possible lengths. The visual observation of the morphology from simulations and analysis of $S(k)$ peaks are used to identify the type of nanostructure. The peaks in the

dependence of C_v on T^* are used to determine the ODT and OOT temperatures.

Previously [13], we studied the $A_x B_{40} A_{40-x}$ series with $x = 1$–3, but for this study we mostly use a longer triblock chain from the $A_x B_{48} A_{48-x}$ series and model the $A1BA2$ chain by a coarse-grained lattice chain of length 96, consisting of two types of segments, using the following asymmetric sequences:

(1) $A_1 - B_{48} - A_{47}$,
(2) $A_2 - B_{48} - A_{46}$,
(3) $A_3 - B_{48} - A_{45}$,

which indicates that we have the same fraction of A and B within the chain (50:50 A:B), but the $A1$ block is much shorter than the $A2$ block. The chains are placed on a fcc $96 \times 48 \times 48$ lattice with the usual boundary conditions, and at a selected parameter, we take the $96 \times 96 \times 96$ and $80 \times 40 \times 40$ lattices. Those lattice sites which are not filled with triblock chains are populated with a selective solvent, either of type A or of type B. The copolymer volume fraction (that is, the fraction of lattice sites occupied by a copolymer) is denoted by Φ. Specifically, we consider the triblock systems as follows:

(1) $A1BA2$ triblocks in the selective A solvent with the $\Phi = 0.7$, $\Phi = 0.8$, and $\Phi = 0.9$ copolymer volume fractions,
(2) pure $A1BA2$ melt ($\Phi = 1.0$),
(3) $A1BA2$ triblocks in the selective B solvent with the $\Phi = 0.7$, $\Phi = 0.8$, and $\Phi = 0.9$ copolymer volume fractions.

III. RESULTS

From previous studies of the $A1BA2$ melts it is well known that significantly below the order-disorder transition temperature the short $A1$ blocks are localized within the B domain, far away from the A/B interface due to an entropic advantage. Despite being counterintuitive from the point of view of the internal energy minimization, this effect is well known from experiment [30], theory [16,31], and simulation [28,32,33]. What was not realized until recently [13], however, was that the $A1$ blocks within the B domains can further self-assemble upon cooling into spatially ordered micelles, referred to as interstitial micelles as shown in Fig. 1. The IMs were found to be stable at very low temperatures (strong segregation) and short $A1$ blocks (note that low fractions of the $A1$ block in the triblock chain require long copolymer chains in lattice simulation). However, long chains and low temperatures pose a considerable challenge for equilibration (and thus the IM formation) in copolymers because the relevant relaxation times become prohibitively long. It is therefore difficult to observe the IMs in simulation but also in potential experiments which were to confirm the existence of stable IMs. It worth reiterating that the IMs were not observed experimentally so far, according to our best knowledge. In this paper we extend the previous study [13] to solutions of $A1BA2$ in both A and B selective solvents for Φ's from 0.7 to 1.0.

It is obvious that the short A block can be localized either in the A domain or in the B domain. As it turns out if they are in the A domain, they tend to be localized near the A/B interface due to heavy enthalpic weight of the long B chain (there is a significant enthalpic penalty for the presence of the long B chain in the A domain). If, on one hand, the short A block is localized in the B domain (due to a entropic advantage), there is no enthalpic penalty for the long B block to be statistically localized in the middle of the B domain. Therefore the short A blocks can be roughly divided into those which are close to the interface and those which are in the B domain. The temperature at which the short A blocks are equally distributed into the interface and the B domain can be identified (see Fig. 2), and it is referred in this paper as the IDC temperature $T^*_{\rm IDC}$. Thus, below this temperature, most short A blocks are localized in the B domain, which may further lead into the interstitial micelles' formation. For pure melts ($\Phi = 1$) the $T^*_{\rm IDC}$ increases with increasing the short A block as indicated in Fig. 2(a) for the 1-48-47, 2-48-46, and 3-48-45 triblock chains. The $T^*_{\rm ODT}$ for the same series decreases with increasing x for the series $x - 48\text{-}(48 - x)$; $T^*_{\rm ODT} = 43$, 37, and 33 for $x = 1$–3, respectively (as also shown in Fig. 4). For the 4-48-44 melt we do not observe the $T^*_{\rm IDC}$, which means that a fraction of the short A blocks in the B domain never exceeds 50%, which can be attributed to a relatively high enthalpic cost of placing a block consisting of four A segments into the B domain. It is also worthwhile to notice that the $T^*_{\rm IDC}$ increases with the increasing total fraction of A segments (that is, including both the chain segments and the solvent segments) as shown in Fig. 2(a). This will also be the relevant trend for the interstitial micelles' formation. In Fig. 2(b), on the other hand, we show the reduced interface-domain crossover temperatures $T^*_{\rm IDC}/x$, illustrating the extent to which the curves of Fig. 2(a) collapse when divided by the length of the short A block.

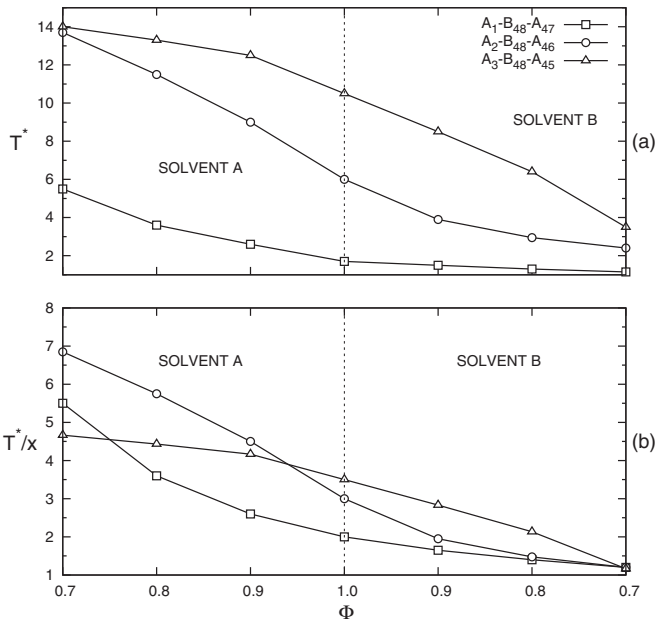

FIG. 2. (a) The interface-domain crossover temperature $T^*_{\rm IDC}$ and (b) the reduced interface-domain crossover temperature $T^*_{\rm IDC}/x$ as a function of copolymer volume fraction for the $A1BA2$-A solution (left-hand side) and the $A1BA2$-B solution (right-hand side). The $A_1 - B_{48} - A_{47}$ triblock is indicated by open squares, the $A_2 - B_{48} - A_{46}$ triblock is indicated by open circles, and the $A_3 - B_{48} - A_{45}$ triblock is indicated by open triangles. Similarly, $x = 1$, 2 or 3 for the $A_1 - B_{48} - A_{47}$ triblock, the $A_2 - B_{48} - A_{46}$ triblock, and the $A_3 - B_{48} - A_{45}$ triblock, respectively.

In Fig. 3, we summarize the main findings of this paper, concerning IMs, by indicating their regions of stability, which are the areas between the solid lines shown in the (T^*,Φ) phase diagrams as shown for different triblock solutions. In contrast to the results for pure melt with an equal fraction of A and B, which yielded only lamellar nanostructures, in this study we observe nonlamellar nanostructures as the selective solvent (either A or B) is added. In particular, for the $A_1 - B_{48} - A_{47}$ solution we observe layers in the region where IMs are stable, for the $A_2 - B_{48} - A_{46}$ solution we can see perforated layers, and for the $A_3 - B_{48} - A_{45}$ solutions we can see spatially ordered cylinders as indicated by the insets in Fig. 3. It is worthwhile to notice that, if the A solvent is added, the solution contains more segments of type A, whereas if the B solvent is added, the segments of type B are in the majority. In Figs. 3(a) and 3(b) we observe that, for $A_1 - B_{48} - A_{47}$ and $A_2 - B_{48} - A_{46}$ solutions, that is, for very short $A1$ blocks, the temperature at which the IMs are formed (upper solid line) increases as the A solvent is added and decreases as the B solvent is added. This may be interesting for the experimental search of IMs that, by adding a solvent which is miscible with terminal blocks, may yield IMs at higher temperatures. We can also observe that the IMs are stable at significantly higher temperatures for the $A_2 - B_{48} - A_{46}$ solution than those for the $A_1 - B_{48} - A_{47}$ and $A_3 - B_{48} - A_{45}$ solutions, which means that there is, most likely, an optimal fraction of $A1$ for the formation of IMs.

In Fig. 4 we show the full phase diagram which also contains ODTs and OOTs and indicates a variety of stable nanostructures, such as layers (L), perforated layers (PL), spatially ordered cylinders (C), bicontinuous nanostructures (B),

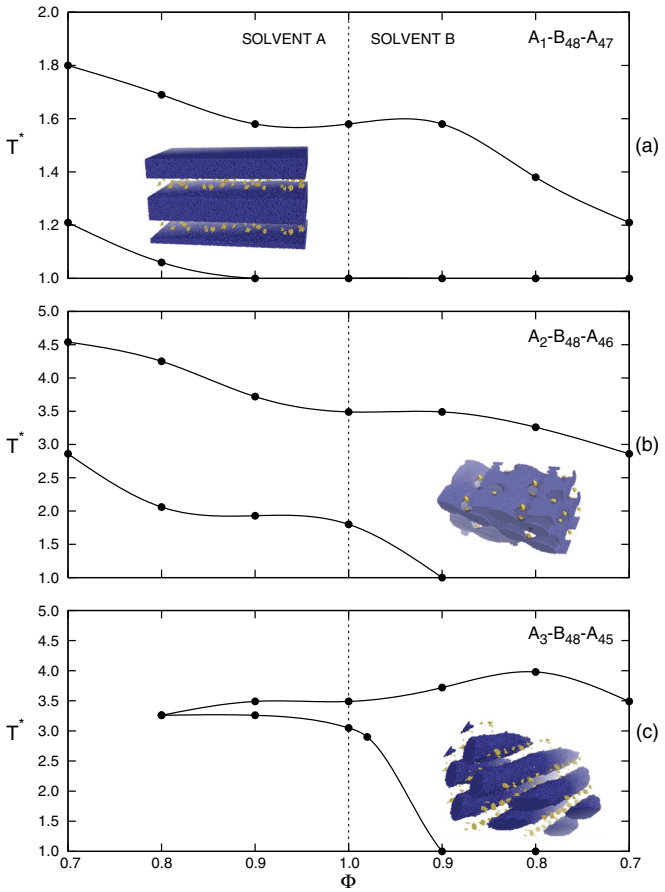

FIG. 3. Interstitial micelles are stable between the solid lines which are shown as a function of copolymer volume fraction Φ in the selective A solvent and B solvent and the reduced temperature T^* (pure melt is at $\Phi = 1$). Individual figures refer to the following $A1BA2$ triblock copolymer solutions: (a) $A_1 - B_{48} - A_{47}$, (b) $A_2 - B_{48} - A_{46}$, and (c) $A_3 - B_{48} - A_{45}$. The inset snapshots indicate (a) layers, (b) perforated layers, and (c) spatially ordered cylinders with morphologies formed by the $A2$ block shown in the blue (dark gray) color. The $A1$ blocks are shown in yellow (light gray) and are visible as interstitial micelles and dangles within the B domain or dangles at the A/B interface. The B blocks and solvent molecules are not shown for clarity.

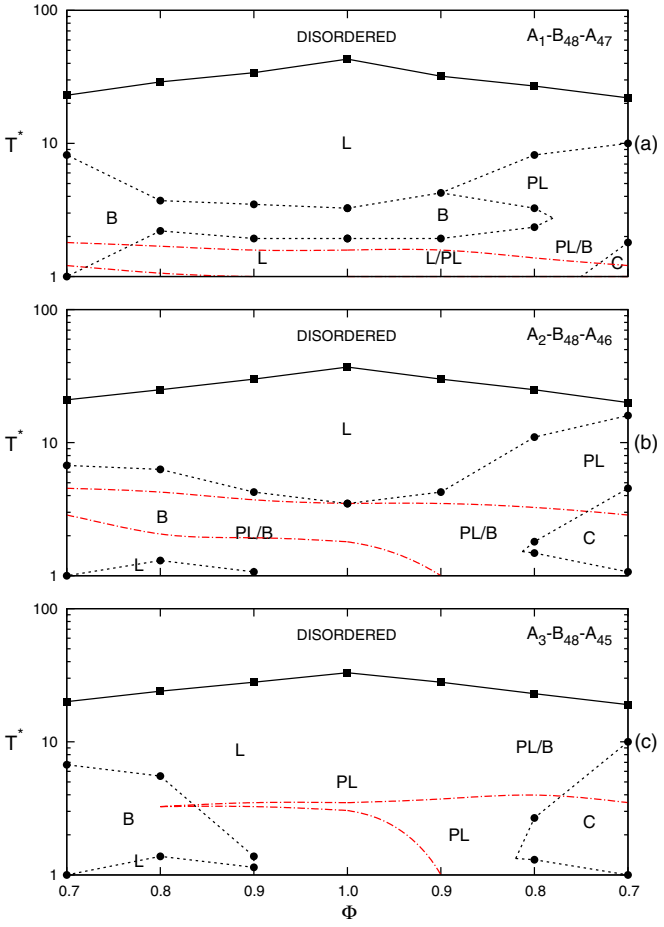

FIG. 4. Phase diagrams as a function of the triblock copolymer volume fraction Φ in the selective solvent of either type A (on the left-hand side) or type B (on the right-hand side) and temperature T^*. Individual figures refer to the following triblock chains: (a) $A_1 - B_{48} - A_{47}$, (b) $A_2 - B_{48} - A_{46}$, and (c) $A_3 - B_{48} - A_{45}$. A logarithmic scale on the T^* axis is used for enhanced clarity. Order-disorder and order-order lines are shown as solid and dashed lines, respectively. L indicates layers, C indicates spatially ordered cylinders, PL indicates perforated layers, B represents the bicontinuous nanostructure, and B/PL means that we observed both B and PL structures. In addition, we mark the borders of the region in which the interstitial micelles are stable by red dashed-dotted lines which correspond to the solid lines shown in Fig. 3.

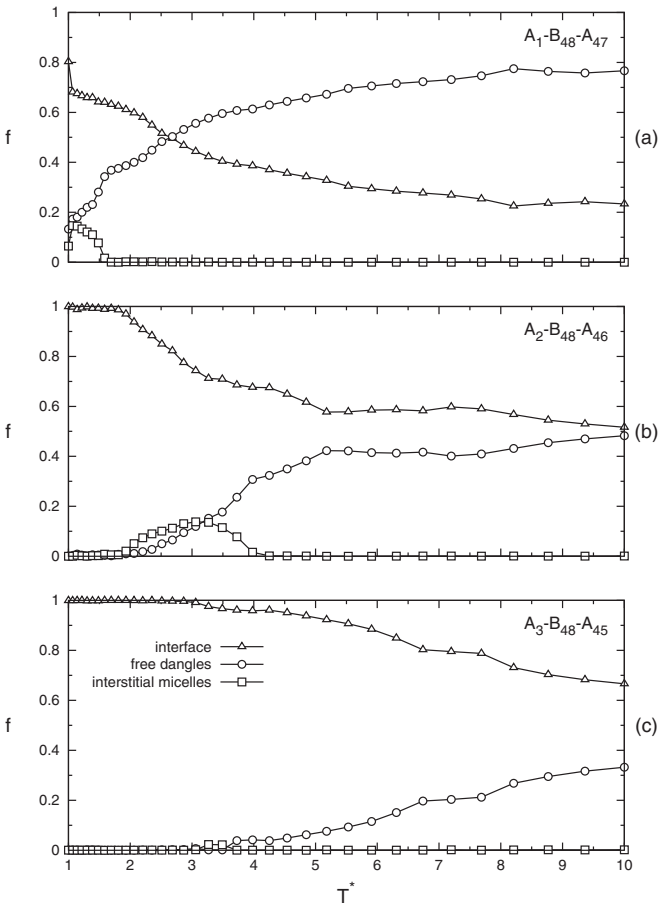

FIG. 5. A fraction of $A1$ blocks which form the interstitial micelles (squares), which form free dangles (circles), and which are located at the A/B interface (triangles) for the $A1BA2$ solution in the selective A solvent ($\Phi = 0.9$) and the following triblock chains: (a) $A_1 - B_{48} - A_{47}$, (b) $A_2 - B_{48} - A_{46}$, and (c) $A_3 - B_{48} - A_{45}$.

and mixed nanostructures PL/B. We can see how the the IM stability range is related to the order-disorder transition temperature. Again the ODT temperature is at the closest distance to the stable IMs for the $A_2 - B_{48} - A_{46}$ solution in the selective solvent of type A at $\Phi = 0.7$. Thus the possible strategy to find stable IMs is as follows:

(1) Find an optimal fraction of $A1$ which yields an IM at the highest temperature using theory (such as self-consistent field theory) and simulations.

(2) Synthesize the corresponding $A1BA2$ triblock chains.

(3) Find a solvent which is miscible with terminal blocks $A1$ and $A2$.

(4) By both adding this solvent and cooling the system try to induce the IM formation.

Next, we present some selective and detailed results indicating the fraction of $A1$ blocks which contribute towards the formation of interstitial micelles. First, in Fig. 5 we show the relative fractions of $A1$ blocks as a function of T^* for the (a) $A_1 - B_{48} - A_{47}$, (b) $A_2 - B_{48} - A_{46}$, and (c) $A_3 - B_{48} - A_{45}$ solutions with the A solvent at $\Phi = 0.9$. Fractions of those $A1$ blocks which are located at the A/B interface are indicated by triangles, those that form free dangles of $A1$ located in the B domain are indicated by circles, and finally those that form IMs are indicated by squares. For $A1$ blocks located at the A/B interface, we do differentiate between bridges (the middle B block anchored at different A domains) and loops (the middle B block anchored at the same A domain). We can clearly see that whereas the $A_2 - B_{48} - A_{46}$ solution in the A solvent yields the broad temperature window for the IM stability (region where the fraction of the IM is clearly different from zero), the $A_1 - B_{48} - A_{47}$ solution in the A solvent produces IMs at significantly lower temperatures and the observed temperature window of stability is narrower (this may also be due to sluggish relaxation at lower temperatures). For the $A_1 - B_{48} - A_{47}$ solution in the A solvent (at $\Phi = 0.9$), on the other hand, we do not observe IMs.

Finally it has to be recognized that, for the simulated solutions in this paper, we do not observe any indications of macrophase separation. This is consistent with the fact that solutions of symmetric block copolymers are known to be stable [12,34,35] (even at a very strong segregation regime) with respect to macrophase separation for Φ's which are greater than 0.5 and a transition to a disordered micellar solution is observed for Φ's which are smaller than approximately 0.2 [12] (note that $\Phi = 0.2$ is well beyond the scope of this study).

IV. CONCLUSION

To summarize, we simulated selective $A1BA2$-A and $A1BA2$-B triblock solutions using a Monte Carlo lattice method. The spatially ordered interstitial micelles were formed from the minority $A1$ blocks within the B-block domain as a result of an entropic effect. We investigate the stability of the IMs as a function of triblock volume fraction in a selective solvent of either type A or type B. The main finding is that adding a selective solvent of type A shifts the stability of the IMs into significantly higher temperatures, which may provide a pathway towards experimental studies of interstitial micelles in real triblock solutions, such as, for example, the polystyrene-polyisoprene-polystyrene triblock. We also find that adding a selective solvent (either A or B) gives rise to a more complex phase behavior with the nanodomains ordered into a variety of nonlamellar morphologies for temperatures and compositions at which the IMs are stable.

ACKNOWLEDGMENTS

Grant No. DEC-2012/07/B/ST5/00647 (S.W. and M.B.) of the Polish NCN and Grant No. DEC-2013/11/B/ST3/04190 (S.J.) of the Polish NCN are gratefully acknowledged. A significant part of the simulations was performed at the Poznan Computer and Networking Center (PCSS). We also acknowledge fruitful discussions with Professor R. Spontak and Dr. K. Mineart.

[1] I. W. Hamley, *The Physics of Block Copolymers* (Oxford University Press, New York, 1998).

[2] *Developments in Block Copolymer Science and Technology*, edited by I. W. Hamley (Wiley, Chichester, U.K., 2004).

[3] R. B. Thompson, V. V. Ginzburg, M. W. Matsen, and A. C. Balazs, Science **292**, 2469 (2001).
[4] F. S. Bates, M. A. Hillmyer, T. P. Lodge, C. M. Bates, K. T. Delaney, and G. H. Fredrickson, Science **336**, 434 (2012).
[5] L. Wu, T. Lodge, and F. Bates, Macromolecules **37**, 8184 (2004).
[6] T. Lodge, Macromol. Chem. Phys. **204**, 265 (2003).
[7] J. Lee, N. Balsara, A. Chakraborty, R. Krishnamoorti, and B. Hammouda, Macromolecules **35**, 7748 (2002).
[8] J. Wang, M. Müller, and Z.-G. Wang, J. Chem. Phys. **130**, 154902 (2009).
[9] C. Zhou, M. Hillmyer, and T. Lodge, Macromolecules **44**, 1635 (2011).
[10] K. Hanley, T. Lodge, and C.-I. Huang, Macromolecules **33**, 5918 (2000).
[11] F. A. Detcheverry, D. Q. Pike, P. F. Nealey, M. Müller, and J. J. de Pablo, Phys. Rev. Lett. **102**, 197801 (2009).
[12] T. Lodge, B. Pudil, and K. Hanley, Macromolecules **35**, 4707 (2002).
[13] S. Wołoszczuk, K. P. Mineart, R. J. Spontak, and M. Banaszak, Phys. Rev. E **91**, 010601 (2015).
[14] H. Watanabe, T. Sato, K. Osaki, M. L. Yao, and A. Yamagishi, Macromolecules **30**, 5877 (1997).
[15] L. Kane, D. A. Norman, S. A. White, M. W. Matsen, M. M. Satkowski, S. Smith, and R. J. Spontak, Macromol. Rapid Commun. **22**, 281 (2001).
[16] M. W. Matsen and R. B. Thompson, J. Chem. Phys. **111**, 7139 (1999).
[17] M. Banaszak, S. Wołoszczuk, T. Pakula, and S. Jurga, Phys. Rev. E **66**, 031804 (2002).
[18] M. Nguyen-Misra and W. L. Mattice, Macromolecules **28**, 1444 (1995).
[19] A. Gauger, A. Weyersberg, and T. Pakula, Makromol. Chem., Theory Simul. **2**, 531 (1993).
[20] A. Weyersberg and T. A. Vilgis, Phys. Rev. E **48**, 377 (1993).
[21] T. Pakula, K. Karatasos, S. H. Anastasiadis, and G. Fytas, Macromolecules **30**, 8463 (1997).
[22] T. Pakula, in *Simulation Methods for Polymers*, edited by M. J. Kotelyanskii and D. N. Thedorou (Dekker, New York, 2004), Chap. 5.
[23] N. Metropolis, A. W. Rosenbluth, M. N. Rosenbluth, A. H. Teller, and E. Teller, J. Chem. Phys. **21**, 1087 (1953).
[24] R. H. Swendsen and J. S. Wang, Phys. Rev. Lett. **57**, 2607 (1986).
[25] D. J. Earl and M. W. Deem, Phys. Chem. Chem. Phys. **7**, 3910 (2005).
[26] P. Knychała, M. Dzięcielski, M. Banaszak, and N. P. Balsara, Macromolecules **46**, 5724 (2013).
[27] G. H. Fredrickson, *The Equilibrium Theory of Inhomogeneous Polymers*, International Series of Monographs on Physics Vol. 134 (Oxford University Press, Oxford, 2007).
[28] S. Woloszczuk, M. Banaszak, and R. J. Spontak, J. Polym. Sci. B **51**, 343 (2013).
[29] P. Knychała, M. Banaszak, and N. P. Balsara, Macromolecules **47**, 2529 (2014).
[30] M. W. Hamersky, S. D. Smith, A. O. Gozen, and R. J. Spontak, Phys. Rev. Lett. **95**, 168306 (2005).
[31] M. W. Matsen, J. Chem. Phys. **113**, 5539 (2000).
[32] S. Woloszczuk and M. Banaszak, Eur. Phys. J. E **33**, 343 (2010).
[33] S. S. Tallury, K. P. Mineart, S. Woloszczuk, D. N. Williams, R. B. Thompson, M. A. Pasquinelli, M. Banaszak, and R. J. Spontak, J. Chem. Phys. **141**, 121103 (2014).
[34] M. Banaszak and M. Whitmore, Macromolecules **25**, 3406 (1992).
[35] S. Woloszczuk, M. Banaszak, P. Knychala, and M. Radosz, Macromolecules **41**, 5945 (2008).